Plasticity of Neonatal Neuronal Networks in Very Premature Infants: Source Localization of Temporal Theta Activity, the First Endogenous Neural Biomarker, in Temporoparietal Areas

L. Routier,[1,2] M. Mahmoudzadeh,[1] M. Panzani,[1] H. Azizollahi,[1] S. Goudjil,[1,3] G. Kongolo,[1,3] and F. Wallois [1,2]*

[1]*Inserm U 1105, University of Picardie Instead of Picardy, Amiens University Hospital, Amiens, France*
[2]*Pediatric Nervous System Investigation Unit, Amiens University Hospital, Amiens, France*
[3]*NICU Amiens University Hospital, Amiens, France*

Abstract: Temporal theta slow-wave activity (TTA-SW) in premature infants is a specific signature of the early development of temporal networks, as it is observed at the turning point between non-sensory driven spontaneous local processing and cortical network functioning. The role in development and the precise location of TTA-SW remain unknown. Previous studies have demonstrated that preterms from 28 weeks of gestational age (wGA) are able to discriminate phonemes and voice, supporting the idea of a prior genetic structural or activity-dependent fingerprint that would prepare the auditory network to compute auditory information at the onset of thalamocortical connectivity. They recorded TTA-SW in 26–32 wGA preterms. The rate of TTA-SW in response to click stimuli was evaluated using low-density EEG in 30 preterms. The sources of TTA-SW were localized by high-density EEG using different tissues conductivities, head models and mathematical models. They observed that TTA-SW is not sensory driven. Regardless of age, conductivities, head models and mathematical models, sources of TTA-SW were located adjacent to auditory and temporal junction areas. These sources become situated closer to the surface during development. TTA-SW corresponds to spontaneous transient endogenous activities independent of sensory information at this period which might participate in the implementation of auditory, language, memory, attention and or social cognition convergent and does not simply represent a general interaction between the subplate and the cortical plate. *Hum Brain Mapp 38:2345–2358, 2017.*

Key words: development; endogenous activity; high density EEG; plasticity; premature

INTRODUCTION

The formation of neural networks in the foetus that participate in integrating sensory information is a key element of neuronal development and depends on intimate interactions between genetically determined guidance and activity-dependent refinement of synaptic connections [O'Leary et al., 2007; Tritsch and Bergles, 2010]. Spontaneous correlated activity is a ubiquitous feature of the developing nervous system, and is thought to provide a robust source of

*Correspondence to: F. Wallois, Inserm U 1105, EFSN pédiatriques, CHU Amiens, Ave Laennec, Salouel, 80054 Amiens Cedex, France. E-mail: fabrice.wallois@u-picardie.fr
The authors declare that they have no conflicts of interest.
Received for publication 9 July 2016; Revised 6 January 2017; Accepted 8 January 2017.
DOI: 10.1002/hbm.23521
Published online 23 January 2017 in Wiley Online Library (wileyonlinelibrary.com).

depolarization prior to maturation of neural circuits [Feller, 2012]. Even before sensory structures become functional, endogenous mechanisms induce cortical bursts of spontaneous activities separated by long quiescent periods. This spontaneous activity in the developing auditory system is necessary for neuronal survival and for refinement and maintenance of tonotopic maps in the brain [Tritsch and Bergles, 2010]. In different functionalities (visual, somatosensory and auditory), some spontaneous activities are independent of all sensory experiences preceding the emergence of visual, auditory and somatosensory abilities, suggesting that isolated neocortical neuronal networks with no sensory inputs are able to generate spontaneous oscillatory patterns and may represent a template for the formation of early functional neuronal ensembles [see Kilb et al., 2011 for review].

At this stage of development, brain innervation is dual, consisting of the subcortical plate and the developing cortical plate. The cortical system of very young preterm infants is therefore on the verge of transition from endogenous spontaneous processing to sensory-expectant functioning [Kostovic and Judas, 2010]. Synaptic mechanisms are still largely immature in these infants [Moore et al., 2011]. From 20 weeks of gestational age (wGA) onward, *in vitro* subplate activity of infants consists of bursts of action potentials separated by quiescent periods during which stimulation of thalamic afferents may trigger stimulus-dependent action potentials [Moore et al., 2011]. Before 26 wGA, the subplate is connected with the quiescent thalamocortical afferents with which they establish the first synapses [Kostovic and Judas, 2010; Kostovic et al., 2015; Zhao et al., 2009]. The subplate progressively involutes from 28 to 32 wGA and almost completely disappears at the end of the first postnatal year [Judas et al., 2013; Kostovic et al., 2011]. The activity of this transitional innervation by the subcortical plate could participate in the development of the plasticity and functionality of the cortical plate [Ayoub and Kostovic, 2009; Kostovic and Judas, 2010; Kostovic et al., 2015; Moore et al., 2011]. Data obtained from *in vitro* thalamocortical slices are in favour of an active role of the subplate in the generation of spontaneous cortical activity in the auditory system [Zhao et al., 2009].

These results in animals and humans underlie the rapid dynamics of the development of sensory cortical networks including auditory networks. Nevertheless, NIRS and ERP studies in very premature infants, from 28 wGA onward, suggest that the functional capabilities are much more mature than previously described [Mahmoudzadeh et al., 2013, 2016]. Only limited human data are available to assess the temporal and spatial organization of these endogenous sensory-independent mechanisms, described in animals during neurodevelopment. Most studies were performed on premature infants aged over 28 wGA [Chipaux et al., 2013; Colonnese et al., 2010; Milh et al., 2007], that is, at a time when thalamic afferents already connect with cortical plate neurons [Kostovic and Judas, 2010], providing sensory inputs for auditory discrimination, for example Mahmoudzadeh et al. [2013, 2016].

Noninvasive assessment of the functional dynamics of brain maturation in preterm infants is mainly based on electroencephalographic analysis. The dynamics of maturation of neural networks in premature infants are characterized by discontinuity in neuronal network activities and the appearance of specific neural biomarkers [Lamblin et al., 1999; Wallois, 2010]. Transient frontal activities [24–27 wGA], temporal theta activity coalescent with slow-wave activity (TTA-SW) [24–32 wGA], delta brushes [30–36 wGA] and "encoches frontales" [34–42 wGA] are successively observed. All of these activities are transient successive generators that appear and disappear during early development in different brain areas. In the temporal areas, TTA-SW are recorded from 24 to 25 wGA onward, independently on both hemispheres and only over temporal structures, while the onset of delta brushes is delayed until 28 wGA with a more widespread distribution [Anderson et al., 1985; Chipaux et al., 2013; Colonnese et al., 2010; Hughes et al., 1987; Milh et al., 2007]. TTA-SW arise with relatively low amplitude. Then, after reaching maximum amplitude and frequency around 28 wGA, their amplitudes gradually decrease and they progressively disappear around the age of 32 wGA during quiet sleep [Biagioni et al., 1994; Lamblin et al., 1999; Vecchierini et al., 2003, 2008], while auditory stimuli generate long-latency cortical responses [Mahmoudzadeh et al., 2013, 2016].

In the foetus or premature newborn, the cochlea is functional by 23 wGA. By the 24th to 25th weeks of foetal life, most auditory brainstem neurons are packed with filaments, and their processes are recognizable as immature dendrites [Moore and Linthicum, 2007].

The first early brainstem auditory evoked potentials can be recorded at least by 25 wGA with different latencies and shapes from those observed in adults, underlining the immaturity of the solicited brainstem networks [Amin et al., 1999]. At the beginning of the third trimester, around the 27th foetal week, the first weak myelin staining is observed in the cochlear nerve between the cochlea and the brainstem [Moore and Linthicum, 2007]. The cortical networks of language exhibit early characteristics of maturity relatively early during development. In fact, the neuronal assemblies of neurons involved in the processing of linguistic information, although still immature in premature infants, use strategies from the age of 28 wGA in response to linguistic stimuli similar to those solicited in adults (habituation mismatch) [Mahmoudzadeh et al., 2016] in brain areas similar to those involved in adult networks (Brocca, Wernicke, planum temporale) [Mahmoudzadeh et al., 2013]. As observed in the visual system, these early networks in the auditory system suggest at least partial anatomical and functional genetic endowment, which might participate in the establishment of early feature maps that initially arise independently of any electrical activities [Crowley and Katz, 2000; Kilb et al., 2011]. Subsequently, as in visual systems, electrical activity is likely to refine the functionality of these auditory pathways [Chiu and Weliky, 2001; Weliky and Katz, 1999].

TABLE I. Clinical data of the neonates by age-group

	Population	26–30 wGA	30–32 WGA
HD EEG			
Number of premature infants	13	5	8
Gestational age at birth (week)		26.7 ± 1.3	28.7 ±1.3
Birth weight (g)		838 ± 189.6	1049.4 ± 243
Mean age at the time of HD EEG (weeks)		28.8 ± 0.9	31 ± 0.6
Mean weight at the time of HD EEG (g)		1088 ± 183.6	1273.8 ± 222.2
Male/Female (%)		60%/40%	25%/75%
Head circumference at the time of HD EEG (cm)		24.6 [23–27]	27 [24.5–30.5]
LD EEG			
Number of premature infants	15	9	6
Gestational age at birth (week)		25.2 ± 1.2	28.9 ± 1.2
Birth weight (g)		737.2 ± 180.5	1229.2 ± 28.7
Mean age at the time of LD EEG (weeks)		26.17 ± 1.02	29.9 ± 0.7
Mean weight at the time of LD EEG (g)		817.5 ± 173.4	1166 ± 231.6
Male/Female (%)		78%/22%	33%/67%

These initial immature circuits develop early during intrauterine life prior to any sensory stimuli. TTA-SW activities appear at a key point in the development, simultaneously with implementation of the functionality of the auditory pathways, at a time when thalamic afferents are still waiting in the subplate before invading the cortical plate from 28 wGA [Kostovic and Judas, 2010; Kostovic et al., 2015; McAllister, 1999; Zhao et al., 2009]. Unlike delta brushes, TTA-SW are highly specific to temporal areas and have never been recorded over other cortical structures.

The objective of this work was to clarify the spatial organization of these specific TTA-SW to noninvasively assess, at an early stage of development in humans, their possible implications in the implementation of cortical language-networks, independently of auditory stimuli.

To achieve this objective, we first used Low-Density Electroencephalography (LD-EEG) to demonstrate that TTA-SW were independent of auditory stimuli. Source localization of these TTA-SW was then performed using High-Density EEG (HD-EEG) with 40–64 channels in two groups of premature infants (26–30 wGA and 30–32 wGA) in order to localize the generators. Our results were also controlled for different tissue conductivities, head models and methods of source localization. The dual innervation of the brain at this stage of development was also carefully taken into account.

MATERIAL AND METHODS

Participants

This retrospective study was based on High-Density ElectroEncephaloGraphy (HD-EEG, 40–64 electrodes mean: 48.7) analysis of 13 healthy premature infants (Table I) and Low-Density ElectroEncephaloGraphy (LD-EEG, 11 electrodes) analysis of other 15 healthy premature infants, recorded for clinical follow-up between the Gestational Ages of 26 and 32 wGA between December 2014 and June 2015. These infants were divided into two groups according to age (26–30 wGA and 30–32 wGA). Although the groups are identical, the mean inside the groups are slightly different for LD and HD EEG recording (LD-EEG: Group 1: 25.2 ± 1.2 wGA: and Group 2: 28.9 ± 1.2 wGA; HD-EEG: Group 1: 26.7 ± 1.3 wGA and Group 2: 28.7 ± 1.3 wGA). EEGs were recorded in the incubator in the Amiens University Hospital neonatal intensive care unit.

All infants had appropriate birth weight, size and head circumference for their term age, an APGAR score greater than 6 at 5 min, normal auditory and clinical neurological assessments and were considered to be at low risk for brain damage. Notably, neurological examination at the time of the recordings had to correspond to corrected gestational age, with no history of abnormal movements. The gestational age, estimated from the date of the last maternal menstruation and ultrasound measurements during pregnancy, was compatible with the cerebral maturation evaluated on the EEG. The temporal dynamics of the occurrence and decay of specific generators of the EEG in premature, such as the TTA-SW the Delta-brush and the frontal transient, together with specific synchronization, discontinuities and amplitude provide the opportunity to clearly define the cerebral maturation according to GA [Andre et al., 2010; Wallois, 2010].

Brain imaging, particularly transfontanelle ultrasound and standard EEG, had to be normal. Exclusion criteria were a corrected age outside the range of 26–32 wGA and/or premature infants with neurological lesions such as intraventricular haemorrhage or any parenchymal malformation and/or pathological standard LD-EEG or HD-EEG.

Study Design and Data Acquisition

Low-density EEG (LD-EEG)

Routine LD-EEG was recorded with Deltamed® amplifiers, with 11 Ag/AgCl surface electrodes placed according

to the International 10–20 system. An additional electrode at position AFz was used as a common earth. Recordings were acquired at a sampling rate of 512 Hz with a 0.3–100 Hz bandpass filter, with an additional notch at 50 Hz. Electrode impedances were kept below 5 kΩ. The electrocardiogram, deltoid electromyogram and oxygen saturation were also monitored together with the video.

High-density EEG (HD-EEG)

As resolution of the inverse problem in EEG source localization in premature infants requires a sufficient number of measurement points, we have developed, for many years, painless caps to support a high-density array of sensors that allow HD-EEG recordings with 64 electrodes in premature infants (Medelopt®) [Roche-Labarbe et al., 2008]. HD-EEG were recorded at the bedside using Ag/AgCl surface electrodes and a nasion reference at a sampling rate of 2,048 Hz, amplified by A.N.T® (Enschede, The Netherlands) and DC-75 Hz filtered. Electrode impedance was kept below 5 kΩ. The number of electrodes (40–64) was determined by the infant's head circumference in order to maintain a regular inter-electrode space (centre-to-centre) of about 1.5 cm. Because of the rapid brain growth at this age, two caps were used to cover the normal range of head circumference (25–33 cm) during this period. In all infants, a minimum of 40 electrodes were placed on the classical 10–10 points adapted to age and supplementary electrodes were placed on intermediate positions according to head circumference. We avoided using a binaural virtual electrode, which would have been located near the regions of interest and which could have potentially contaminated by passive high-amplitude temporal theta activity. Similarly, a virtual reference electrode consisting of the average of the active electrodes would have reintroduced the TTA-SW in other electrodes, particularly because of the low signal encountered during discontinuities in the contralateral hemisphere. Finally, a Laplacian assembly was not necessary because of the high signal-to-noise ratio of theta activity and their occurrence restricted to only a few electrodes.

Effect of Auditory Stimuli on the Occurrence of TTA-SW

To determine whether or not TTA-SW were sensory driven, we evaluated the effect of click stimuli on the occurrence of TTA-SW in a 15 premature infants using the same protocol as that proposed to demonstrate the sensory driven susceptibility of delta brushes over the temporal areas before 35 wGA [Chipaux et al., 2013]. Two loudspeakers were placed inside the incubators (Logitec® 20–20 kHz) 10 cm away from the infant's head. Click stimuli consisted of a 4 ms square signal of 5000 Hz at 70 dB using a pseudo-random design every 20–25 seconds to avoid habituation, during both quiet sleep and active sleep. A total of 120 clicks were delivered to each infant over about 40 minutes. On-line synchronization between the 2 systems was performed via a built-in MATLAB procedure, which provides a marker for each click on the EEG acquisition device. The click stimuli period started 15 minutes after a background activity recording (according to the clinical protocol used in Amiens).

Selection of Temporal Theta Activities in Coalescence with Slow Waves (TTA-SW)

To identify TTA-SW, LD-EEG and HD-EEG were analysed by Coherence 3NT (Deltamed®) and ASA (ANT® Software), respectively. Data were bandpass filtered (0.5–40 Hz) and down-sampled to 512 Hz, as this bandwidth eliminates infra-slow activities [Vanhatalo et al., 2002] and any DC current shift. TTA-SW were selected on the basis of descriptions of EEG features of prematurity [Lamblin et al., 1999]. To be eligible, TTA had to be present over temporal electrodes, in groups of at least 2 and coalescent with a slow wave (SW). TTA had to present a theta frequency between 4 and 7.5 Hz and an amplitude greater than 25 μV [Andre et al., 2010; Lamblin et al., 1999]. The Slow waves were selected if and only if they were immediately preceded by at least 2 selected TTA. TTA-SWs were excluded when a concomitant artefact was present.

Peak detection

TTA and SW were manually and separately selected using a marker positioned on the peak of each TTA and on the peak of each SW activities under the electrode providing the highest signal-to-noise ratio. Selection was performed under blinded conditions by three experienced electrophysiologists (FW, LR, MP) and only TTA and SW identified by all three electrophysiologists were finally selected.

Hemispheric selectivity

For HD-EEG source localization, as the EEG activity of premature infants at this stage of development is characterized by its discontinuity and asynchrony, we carefully selected TTA-SW occurring in only one hemisphere, during a period of discontinuity in the contralateral hemisphere. The same procedure was applied to slow waves coalescent with TTA. TTA-SW source localization was performed separately in each hemisphere. At least 10 TTA-SW were selected on HD-EEG for each premature infant (Fig. 1).

Data Analysis

Effect of auditory stimuli on TTA-SW on LD-EEG

A peristimulus histogram (0.5 s bins) was created in MATLAB, cantered (−10, +10 sec) over time 0 corresponding to the marker of the TTA-SW for each subject. The effect of 100 clicks per patient was analysed. A grand

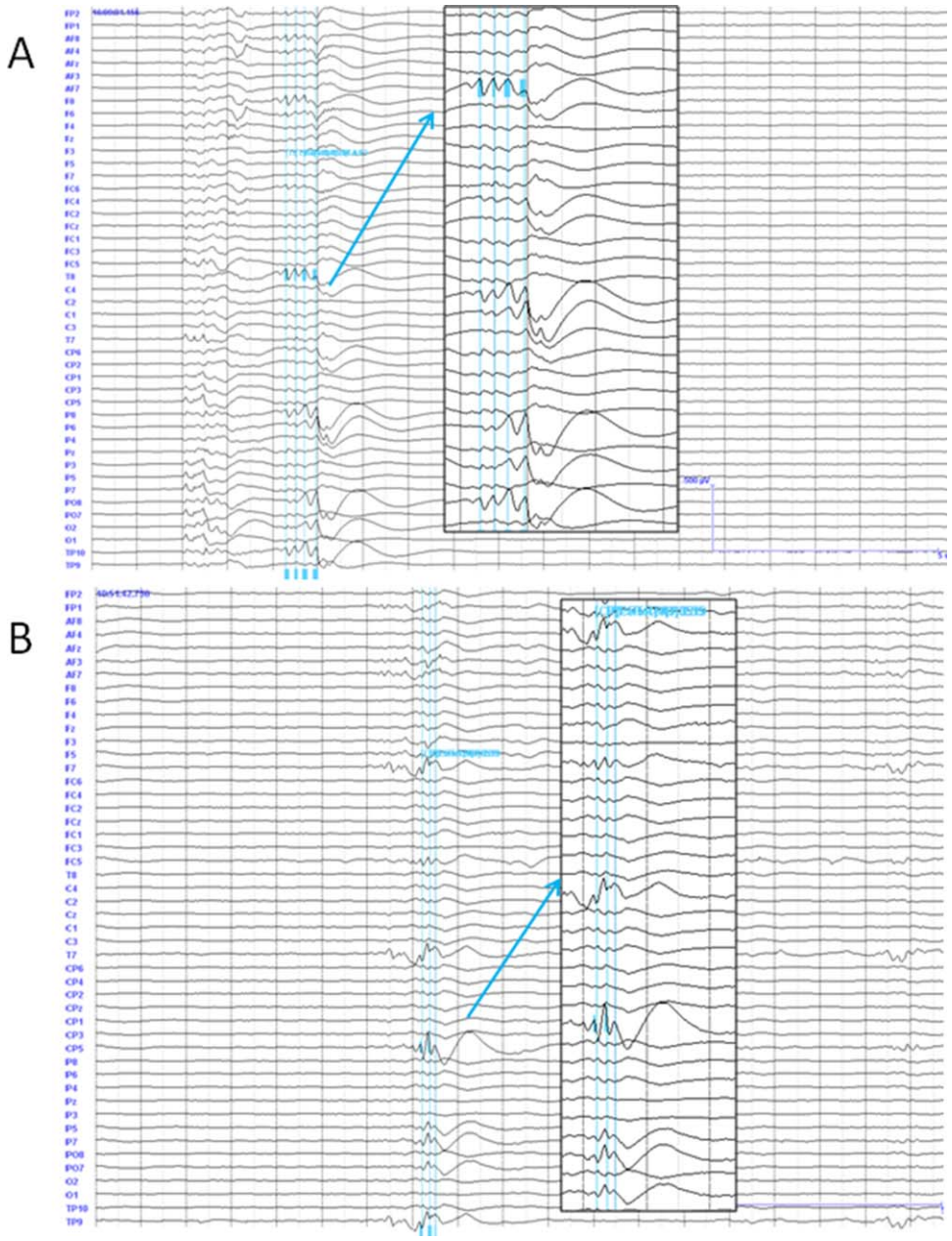

Figure 1.
HD-EEG recorded in premature infants (A: group 1: 26 wGA and B: group 2: 31 wGA) (band-pass: 0.5–40 Hz). The enlargement shows the selection of TTA-SW for each population.

average peristimulus histogram was then plotted for the various subjects.

Statistical analyses were performed with a non-parametric statistical test for paired samples (Wilcoxon test). The −10 to +10 sec around the click stimuli were subdivided in 2 sec interval. The rates of TTA-SW occurrence were analysed according to a baseline reference evaluated from the mean of TTA-SW occurrence during each of the 5 interval preceding the click.

HD-EEG source localization of TTA-SW

The various steps of data analysis are shown in Figure 2.

Creation of head models. In view of the dynamics of head growth at this age, two magnetic resonance imaging (MRI) head models were adapted to the age (T1 (26–30 wGA) and T2 (30–32 wGA)) of the premature infants. Group 1 consisted of infants between 26 and 30 wGA and group 2 consisted of infants between 30 and 32 wGA. To

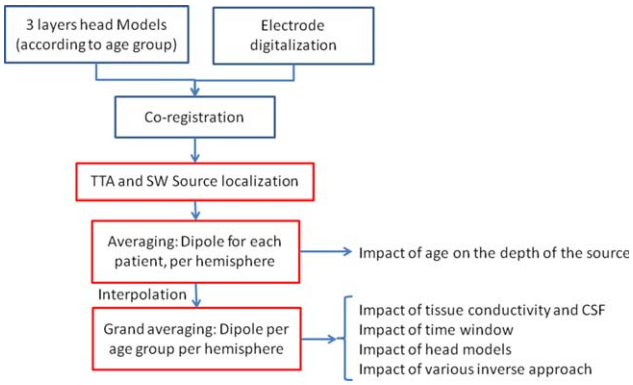

Figure 2.
Block diagram of the various methodological steps for HD-EEG source localization.

eliminate the impact of an inappropriate head model, the results of source localization were verified in a third independent MRI head model [T3 (30 wGA)]. These realistic head models were obtained by segmentation of the various layers in order to delineate the 'air-scalp', 'scalp-skull' and 'skull-brain' interfaces [see Roche-Labarbe et al., 2008 for the segmentation method]. The various tissues were identified by segmentation using a combination of grey-scale thresholding and a region growing algorithm plus three operators: opening, closing, dilation. Although neonates present low grey-scale contrast between various tissues on MRI images, careful thresholding resulted in satisfactory head modelling. A fourth layer was segmented to account for the effect of cerebrospinal fluid (CSF). CSF was extracted by dilation of the brain, thereby reducing the thickness of the skull. These boundary element head models allow a specific conductivity value to be attributed to each layer. During the segmentation process, anatomical markers (nasion, right and left ears) were manually defined on MRI images. These points were automatically included in the head models. Conductivity values identical to those used in adults (scalp: 0.33 S/m, bone: 0.0042 S/m and brain tissue 0.033 S/m) [Cho et al., 2015; Odabaee et al., 2013; Roche-Labarbe et al., 2008] were initially used. Many factors remain unknown, such as the conductivities of immature tissues, the impact of CSF and the presence of the fontanelle in premature infants. Parallel studies conducted in the laboratory [Azizollahi et al., 2016] suggest that the incorporation of a CSF layer is essential in premature infants, as in adults [Ramon et al., 2004; Rice et al., 2013; Vallaghe and Clerc, 2009; Vorwerk et al., 2014]. To minimize the risk of misinterpretation, the impact of bone conductivities with or without CSF on localization of the TTA-SW generators was evaluated (see below). As the impact of the fontanelle is considered to be relatively limited away from the fontanelles [Azizollahi et al., 2016; Gargiulo et al., 2015; Lew et al., 2013; Roche-Labarbe et al., 2008], the fontanelles were not included in our model.

Digitization of EEG electrode positions and coregistration. The position of the electrode setup was obtained after digitization by an infrared method [Koessler et al., 2011] using a phantom adapted to the size of the head outside the incubator. To maintain the same position of the electrodes, the same two mounted caps were used for all children in each group throughout the recording period.

The digitized positions of electrodes were then combined with the head models for each child, by matching with the anatomical markers. After coregistration on the appropriate head models, source localization was performed for each patient and according to each hemisphere.

Source localization methods. Source localization consists of solving the inverse problem by defining the location of the generator using the electrical activity recorded from the surface by scalp EEG electrodes. Several localization methods are available. The sources of the average TTA-SW were estimated by a discrete source localization method (Dipole fitting). The Dipole Fit method is a method of iterative inverse localization providing a unique source with coordinates, amplitude and orientation, based on the assumption that the recorded activity is due to a unique generator located in a limited area. The activity in each area is therefore linked to that of a single dipole [Baillet et al., 2001].

As functional connectivity analysis has suggested that the impact of TTA-SW is limited to small temporal areas [Adebimpe et al., 2016], TTA-SW were assumed to arise from a single source and do not spread in large networks. Single rotating dipoles were therefore used for dipole fitting and were expected to indicate a location close to the cortex. Dipole fitting using rotating dipoles generally provides stable and reliable source localization for the time interval of the event. The orientation and amplitude are determined by the best-fit latency. Source reconstruction solutions were projected onto the original 3D MRI images. For each data set and for the two head models source localization was calculated by using dipole fit on each selected event and then on the average of the events.

Scanning methods used for source localization consider each volume element in the brain area and estimate the probability of the presence of a current dipole in this position. To minimize misinterpretation due to the source localization method used, the dipole fit and Music methods were both considered.

Given the dual innervation of the cortex during this period of development [Kostovic et al., 2011] and to take into account possible involvement of the subcortical plate, we measured the Euclidean distance of TTA-SW relative to the surface of the scalp in each group to evaluate possible changes in the depth of generators according to age, using the equation:

$$D=\sqrt{(x_1-x_2)^2+(y_1-y_2)^2+(z_1-z_2)^2}$$

where D is the Euclidean distance expressed as the square root of the sum of squared differences between x, y and z components for each position.

As the temporal activities occurred in coalescence with a slow wave, suggesting a special temporal relationship between two coupled generators, for which temporal theta activities always precede slow waves, the two generators were therefore localized separately.

Localization of dipoles in each patient

First, to eliminate ultra-slow waves that subtend physiological activities at this period of development and which are related to other mechanisms, 2 and 0.6 Hz high-pass filters were applied for TTA and SW source localization, respectively. Second, for each patient an averaging of the TTA and of the SW was performed separately with a time window around the peak of TTA and SW (−0.3 to +0.8 seconds) which were detected manually. Third, a second time window surrounding the peaks (−70 to 70 ms) was selected.

Then, TTA and SW source localization were carried out using the dipole fit method implemented in ASA® software package (ANT Software, Enschede, The Netherlands) [Zanow and Knosche, 2004] from the average TTA and SW for each patient and for each hemisphere. Secondarily, in order to evaluate the dispersion of the dipoles in each group, a cluster of dipoles in each group of patients and each hemisphere was constructed for TTA and SW and reintroduced into the realistic head model adapted to age.

Data interpolation and localization of dipoles after grand averaging per group

In order to compare data across groups and to perform grand averaging of TTA and SW across patients, a cubic interpolation for each HD-EEG was performed on a 64 virtual electrode setup. To evaluate the errors of source localization due to data interpolation, the positions of the dipoles were checked before and after interpolation. After interpolation, data were grand-averaged over patients per group and per hemisphere. A new time window was selected, as previously described, surrounding the peak of the TTA and SW. Dipole source localization was then performed after grand averaging. To avoid misinterpretation due to the inverse method used, the MUSIC scanning method was also performed to compare source localizations between the two methods using the same time windows and the same head models.

The depth of the dipoles was calculated on the MRI coronal section passing through the dipole, using the coordinates of the dipole and the intersection with the cortex of the line joining the dipole and the cortex following the orientation of the dipole.

The Euclidean distance between these two points was then determined and compared according to the various conditions (age, conductivity, head models).

Impact of Conductivity on the Position of the Source

Changes in bone conductivities

The impact of conductivities was assessed in the group comprising the largest number of preterm infants (Group 2).

As the conductivities of various newborn tissues, including bone, are unknown, we assumed that newborn skull conductivity would be situated between the standard adult value of 0.0042 S/m and the extreme value of cerebral conductivity (0.33 S/m) [Geddes and Baker, 1967; Goncalves et al., 2003; Roche-Labarbe et al., 2008]. Two situations were therefore considered:

- Situation 1: the bone conductivity value corresponds to that described in adults, that is, 0.0042 S/m [Roche-Labarbe et al., 2008].
- Situation 2: as the bone of newborn infants is in the process of ossification, its conductivity is probably higher than that of adults. In order to assess the maximum error due to bone conductivity, we considered an extreme situation in which the bone conductivity is equal to that of other soft tissues: 0.33 S/m (situation 2a) [Roche-Labarbe et al., 2008]. A conductivity value between these two extremes (0.16 S/m) was then applied (situation 2b).

The conductivity value of the scalp and brain tissue were considered to be similar to those used in adults (0.33 S/m) [Cho et al., 2015; Lanfer et al., 2012; Odabaee et al., 2013; Vorwerk et al., 2014].

The positions (x, y, z) of the dipoles were compared according to variations in conductivity. Euclidean distances between the dipoles were calculated for the various conditions.

Impact of cerebrospinal fluid

The CSF is an important layer both in adults [Ramon et al., 2004; Rice et al., 2013; Vallaghe and Clerc, 2009; Vorwerk et al., 2014] and in term neonates [Azizollahi et al., 2016] and probably has a major impact on source localization. To check for errors of source localization related to the use of a 3-layer head model without CSF, a 4-layer head model was computed from the same 3D head model (UCL Head model). To specifically study the impact of inclusion of CSF, the conductivities of the scalp, skull and brain tissues were set at 0.33, 0.0042 and 0.33 S/m, respectively. As CSF conductivity is unknown in preterm infants, we considered 5 conductivity values for CSF, ranging between the conductivity of the skull (0.0042 S/m) and the conductivity of CSF in adults (1.79 S/m) [Cho et al., 2015; Lanfer et al., 2012; Odabaee et al., 2013; Vorwerk et al., 2014].

RESULTS

Effect of Auditory Stimuli on TTA-SW Generation

Click stimuli similar to those used to evoke delta brush activities in preterms before 35 wGA [Chipaux et al., 2013] failed to evoke or induce any increases in TTA-SW

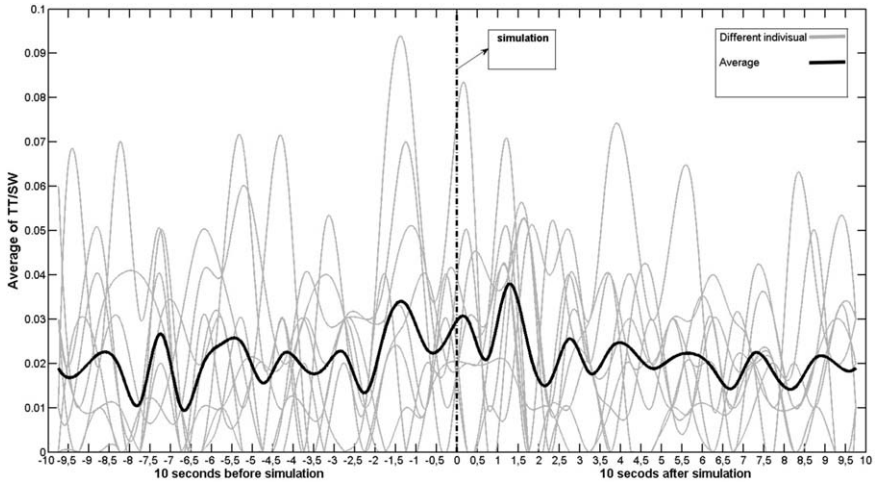

Figure 3.
Effect of click stimuli on the occurrence of TTA-SW (*x*: time in seconds, *y*: number of TTA-SW per 0.5 s). The figure represent the interpolation of the frequency of TTA-SW occurrence within 0.5 s intervals for each subject (grey lines) and the grand average across subjects (dark line)

between 26 and 32 wGA (Fig. 3), demonstrating that TTA-SW are not auditory-driven at this age.

TTA-SW Source Localization

The resulting activities of the two generators (temporal theta activities and slow waves) were localized to the same temporal electrodes on HD-EEG recordings (Fig. 1). Furthermore, as previously described [Lamblin et al., 1999], the amplitude of TTA decreased with age, suggesting an age-related change in the activity or position of the generators.

An average of 68.3 ± 29.6 right TTAs and 84.9 ± 20.6 left TTAs were selected for each premature infant (see Table II). The dipole fit method for each patient using conductivity values of 0.33, 0.0042 and 0.33 S/m for the scalp, skull and brain, respectively, suggested that TTA and SW were subtended by two generators located in the posterior part of the superior temporal sulcus (STS) with an upward orientation directed toward the centre of the brain in each patient (Goodness Of Fit, GOF = 87.7% ± 5.4%). To assess the impact of age, the source localization of clusters of dipoles were analysed according to their Euclidean distance from the surface as a function of age (Table II). On both sides, the dipole positions of TTA were located significantly deeper (*t*-test, $P < 0.0006$) in the youngest infants [26–30 wGA] (group 1: 12.8 ± 3.1 mm vs. Group 2: 6.1 ± 2.8 mm).

Individual data from 64 electrodes were interpolated to represent sources according to a single reference system in each age-group, independently of the number of electrodes used. After evaluating the effect of interpolation (Euclidean distance before and after interpolation: 5.6 ± 8 mm), grand averaging was performed to localize the generators of TTA on age-matched head models (Fig. 4B). Regardless of the group and the side, the dipoles were located in the

TABLE II. Quantitative characteristics of selected activities (Temporal Theta Activities and Slow Waves)

	Population	Group 1	Group 2
Number of electrodes used in HD EEG (M [min–max])	48.6 [40–64]	50.6 [44–64]	47.3 [40–64]
Number of Temporal Theta activities (M ± EM)			
Right	68.3 ± 29.6	39.8 ± 20.2	83.8 ± 35.7
Left	84.9 ± 20.6	79,5 ± 36	79.9 ± 21.7
Total	125.7 ± 40.7	97.2 ± 39	140.6 ± 54.1
Number of Slow Waves (M ± EM)			
Right	15.3 ± 5.2	10.5 ± 0.7	17.8 ± 6.6
Left	15.1 ± 1.7	17.7 ± 2.9	13.8 ± 0.6
Total	15.2 ± 3.1	14.8 ± 3.4	15.4 ± 3.1
Mean distance of the dipoles of the individual TTA from the cortical surface (mm)			
Right dipoles	9.9 ± 4.2	12.6 ± 4.8	7.3 ± 2.6
Left dipoles	7.9 ± 3.9	13.1 ± 1.1	5.3 ± 2.6
Total	8.8 ± 4	12.8 ± 3	6.1 ± 2.8

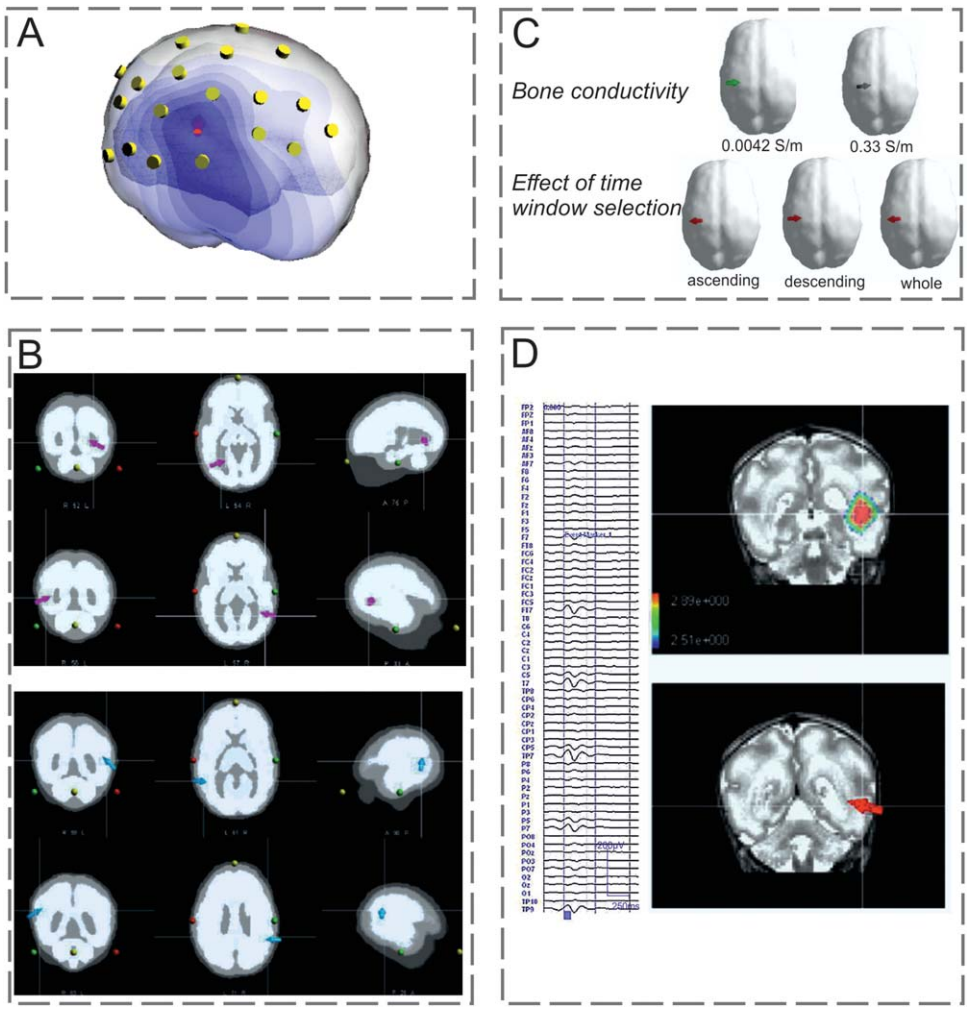

Figure 4.

A: EEG topoplot and dipole of right TTA of a subject in Group 2. B: Source localization of TTA after grand averaging in group 1 (upper panel) and group 2 (lower panel) for left (upper row) and right (lower row) TTA. C: Effect of bone conductivity on source localization (upper row). Effect of time window selection on source orientation (lower row) on TTA in group 2. D: Source localization of TTA in group 2, using a third head model and different source localization methods (dipole fit and Music).

posterior part of the STS below the surface of the cortex. The resulting right and left dipoles after grand averaging were still located deeper for the youngest infants [distance from the surface: left: 15.4 mm and right: 14.0 mm for group 1 vs. left: 11.2 mm and right: 7.8 mm for group 2 (GOF: 94.6% ± 1%)].

Impact of Tissue Electrical Conductivity on Source Localization

As bone conductivity is unknown in preterm infants and could impact on source localization, the effect of bone conductivity (Fig. 4C) was studied on averaged data by measuring the Euclidean distance between the positions of the sources for conductivity values of 0.0042 S/m, 0.16 S/m and 0.33 S/m in the oldest premature infants (group 2). An increase in bone conductivity caused a maximum Euclidian displacement of the source, still located in the posterior part of the STS, of 9.5 mm toward the centre of the cortex (y direction) for conductivity values of 0.0042 versus 0.33 S/m (x = 0.6 mm, y = 9.3 mm, z = −1.8 mm) and a displacement of 9.2 mm for conductivity values of 0.0042 versus 0.16 S/m (x = 0.5 mm, y = 8.9 mm, z = −2.5 mm), while the displacement was only 8 mm for a conductivity of 0.16 versus 0.33 S/m. As expected, the magnitude of the dipole decreased when bone conductivity increased (35.9–27.7 nA for 0.0042 S/m vs. 33 S/m and 35.9–24.6 nA for 0.0042 S/m vs. 0.16 S/m) with no change

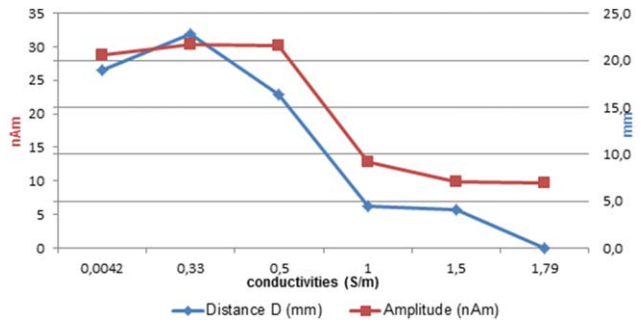

Figure 5.
Impact of CSF on the Euclidian distance and amplitude of the dipole source (reference CSF conductivity: 1.79 S/m).

in orientation. The GOF was similar regardless of bone conductivity values (94.5%, 94.7% and 94.8% for 0.0042, 0.33 and 0.16 S/m, respectively).

To assess the impact of CSF, the head model used for the older infants (group 2) was further segmented into four layers including CSF, with conductivity values ranging from 1.79 S/m (reference CSF conductivity in adults) to .33 S/m [reference brain conductivity in adult (no CSF)] (conductivity of the scalp, skull and brain were kept constant). In all cases, the dipole of group 2 remained located along the STS (GOF: 84.8% ± 5.8%). Including CSF in the model displaced the dipole toward the surface of the brain (y = 20.1 and 33.5 mm for conductivities of 0.33 and 1.79 S/m, respectively) and caused a maximum Euclidian displacement of the source, still located in the posterior part of the STS, of 22.7 mm (x = −9.7, y = 20.1, z = 18.8 for 0.33S/m and x = −6, y = 33.5, z = 37 for 1.79 S/m). As expected, considering the Y direction, the higher the conductivity of CSF, the more the distance from the source to the surface decreased and the more the magnitude of the source decreased (Fig. 5).

Impact of the Time-Window on Source Localization

To ensure that selection of the time window within the TTA did not influence source localization, the source of the generator was localized from the ascending slope, descending slope or the entire period surrounding the TTA (Fig. 4C). TTA source localization was not affected by the time window selected after grand averaging (Table III). Only the orientation of the dipole was reversed according to whether the ascending portion or the descending portion was selected.

TABLE III. Effect of time window selection on the position of TTA source localization

	X	Y	Z	Euclidian distance (mm)
Peak	−9.4	24.2	19.1	
Ascending slope	−9.1	25.1	19.6	1.1
Descending slope	−9.9	24.2	20.2	1.2
Whole period	−9.4	24.7	19.9	0.9

Impact of the Head Model on Source Localization

To ensure that the position of the dipole was independent of the head model, source localization was performed by the dipole fir and MUSIC methods on a third segmented MRI of a 30 wGA premature infant. Analysis by these two methods did not alter the relative positions of the sources with respect to the surface, or their position along the posterior part of the STS (Fig. 4D).

Impact of Various Inverse Approaches on Source Localization

To ensure that source localization was globally independent of numerical methods, the Euclidian distance between the centre of the Music area and the coordinates of the dipoles was evaluated to be about 7 mm (x = −16.8, y = 20.4, z = 0.00 and x = −17.9, y = 26,9, z = −2.9 for Music and dipole fit, respectively. Regardless of the methods used, the source was still located in the posterior part of the STS, although slightly deeper with Music than with Dipole fit (Distance to the surface of the brain: Music: 10 mm, Dipole Fit: 4.4 mm) (Fig. 4D).

DISCUSSION

Regardless of age, conductivities, head models, the mathematical models and the method used to select time-windows for analysis, sources of TTA-SW were located beneath the structures involved in discrimination of phonemes and voices as early as 28 wGA in preterms (Mahmoudzadeh et al., 2013] including STS and planum temporale. These sources became closer to the surface during development, and were always located beneath the cortical plate.

Endogenous TTA-SW Independent of Sensory Inputs

The development of sensory abilities of neural networks depends on successive mechanisms, such as (i) anatomical and functional genetic coding independent of sensory information, (ii) spontaneous endogenous electrical activities independent of sensory information and (iii) finally a refinement of the functionality of the networks by sensory-driven electrical inputs.

TTA-SW generators are therefore active (1) after establishment of peripheral hearing functionality (23 wGA), (2) before or concomitantly with the occurrence of brainstem evoked potentials (25 wGA), (3) before invasion of the cortical plate by thalamic afferents (28 wGA) and (4) before

the appearance of endogenous delta brush generators (28 wGA). The results of this study demonstrate, for the first time, that TTA-SW are not sensory-driven at this period of development.

Spontaneous electrical activities, independent of sensory inputs, are generated throughout the auditory pathway even before the onset of hearing. In the inner ear, before the development of effective auditory function, Kölliker cells located in the cochlea spontaneously depolarize and, in turn, depolarize inner hair cells that promote the emergence of periodic action potentials in spiral ganglion neurons [Kilb et al., 2011; Tritsch et al., 2007; Zhao et al., 2009]. These spontaneous activities appear to be geneticallly encoded and participate in implementation of the final functional organization of the cochlea [Kilb et al., 2011; Tritsch and Bergles, 2010; Tritsch et al., 2007]. At the cortical level, pre-wiring of the structures involved in language processing, anatomical/functional asymmetry [Dubois et al., 2008, 2014; Leroy et al., 2011] and various discrimination abilities [Mahmoudzadeh et al., 2013, 2016] are likely to depend on an initial genetic fingerprint. Endogenous oscillations and waves have been reported in the thalamorecipient auditory cortex in immature animals, with an incidence of 0.4–5 waves/min, and a mean instantaneous firing of 6.4 ± 1.3 Hz similar to that observed for TTA-SW in this study [Kotak et al., 2007, 2012]. These spontaneous auditory cortical activities in rats and gerbils precede the onset of hearing and gradually disappear following the initiation of sound-evoked response when low-frequency sound cues are first perceived [Kotak et al., 2007, 2012]. TTA-SW that are also independent of sensory stimuli at this period of development have the same temporal dynamics as the spontaneous auditory cortical activities in animals. They also gradually decrease in amplitude from 28 to 32 wGA and then progressively disappear following the establishment of thalamocortical connections and the onset of hearing, after or concomitantly with the emergence of long latency cortical evoked responses [Mahmoudzadeh et al., 2013, 2016] and the onset of delta brush generators [Wallois, 2010]. Whether this endogenous activity is derived from peripheral endogenous cochlear waves, as proposed for retinal waves that trigger spindle bursts in the visual cortex, is unknown [Hanganu et al., 2006].

TTA-SW Source Localization

It is currently unknown whether the subplate is the site of the TTA-SW generator. The subplate is a temporary structure that represents most of the foetal forebrain with a maximum thickness around 28–32 wGA and which then gradually decreases [Kostovic and Judas, 2010]. A parallel can be drawn between the progressive decrease of subplate thickness and the position of TTA-SW, which was found to be deeper for the group of younger infants. In addition, together with subplate thickness, the incidence of TTA-SW decreases after 28 wGA [Wallois, 2010]. Unlike the cortical plate, the subplate is an area of early synaptic activity at this stage of development [Moore et al., 2011]. *In vitro*, from 20 and 21 wGA, this structure is able to generate endogenous activities independently of sensory inputs [Lamblin et al., 1999; Moore et al., 2011]. This early activity of the subplate plays a crucial role in the development of the nervous system, with a functional role in the guidance, migration, neuronal differentiation, axonal growth, synaptogenesis and neurotransmitter activation of ionic channels indispensable in the preparation of the future brain functions [Ayoub and Kostovic, 2009; Kostovic et al., 2011; Moore et al., 2011; Ulfig et al., 2000].

The micro-architecture of the subplate neural organization, with neurons oriented perpendicular to the surface of the brain [Sarnat and Flores-Sarnat, 2002], should not result in closed electrical fields not accessible to EEG [Judas et al., 2013; Zhao et al., 2009]. However, while thalamic afferents have not yet completely reached the cortical plate, the subplate plays an intermediate role in the development of the functionality of cortical structures [Zhao et al., 2009] and its axons can activate the still limited number of still migrating cortical neuronal networks, but already oriented perpendicular to the cortical surface and therefore likely to produce dipoles that could be recorded by scalp EEG. Our data are in accordance with recent results from neocortical slice cultures, suggesting that the subplate may act as a pacemaker region to generate network activity [Lischalk et al., 2009]. Several experimental findings support the contribution of subplate neurons to the generation of network oscillations *in vivo*. Current source density analysis of spindle bursts has revealed the generator of these nonspecific early oscillations within the subplate [Yang et al., 2009].

However, very localized appearance of TTA-SW dipoles, regardless of age, adjacent to the STS, the planum temporale and the temporoparietal junction suggests that TTA-SW are related to a very specific feature. They might be involved in the implementation of auditory, language, memory, attention and or social cognition convergent functions [see Carter and Huettel, 2013 for a review], and does not simply represent a general interaction between the subplate and the cortical plate. At the temporal level, data obtained in thalamocortical slices *in vitro* suggest an active role for the subplate in the generation of spontaneous cortical activity in the auditory system [Zhao et al., 2009]. This functional and local specificity of TTA-SW is further supported by the poor functional connectivity of temporal structures with other brain structures in premature infants [Adebimpe et al., 2016].

By analogy with endogenous spontaneous activity in the developing cortex, spontaneous TTA-SW generators would reflect the general properties of the neuronal population interconnected by electrical and chemical synapses [Adelsberger et al., 2005; Conhaim et al., 2011; Garaschuk et al., 2000; Gonzalez-Islas et al., 2010; Shatz et al., 1990; Tritsch and Bergles, 2010; Wong, 1999]. They would therefore

participate in the development of the auditory network, while the original targeting and segregation of inputs in auditory structures would be related to genetically encoded guidance, as described elsewhere. TTA-SW generators are also highly specific to the auditory cortex and differ from delta brushes [Chipaux et al., 2013; Colonnese et al., 2010; Milh et al., 2007] by their frequency content, their time of onset, and their specificity to temporal, temporoparietal junction-related areas only. These features support the idea that different activity patterns (TTA-SW vs. Delta brushes) can sequentially influence different functional attributes or aspects of map refinement, as in retina where some features of waves drive retinotopic refinement while other features drive eye-specific segregation [Xu et al., 2011].

CONCLUSION

Temporal theta activities correspond to a spontaneous transient endogenous activity generated by temporary structures, independent of sensory information at this period of development and well localized to participate in the implementation and future functionality of the entire auditory, language and memory, attention and or social cognition convergent networks.

ACKNOWLEDGMENTS

The authors are grateful to the Amiens university hospital EEG technicians for data acquisition.

REFERENCES

Adebimpe A, Aarabi A, Bourel-Ponchel E, Mahmoudzadeh M, Wallois F (2016): EEG resting state functional connectivity analysis in children with benign epilepsy with centrotemporal spikes. Front Neurosci 10:143.

Adelsberger H, Garaschuk O, Konnerth A (2005): Cortical calcium waves in resting newborn mice. Nat Neurosci 8:988–990.

Amin SB, Orlando MS, Dalzell LE, Merle KS, Guillet R (1999): Morphological changes in serial auditory brain stem responses in 24 to 32 weeks' gestational age infants during the first week of life. Ear Hear 20:410–418.

Anderson CM, Torres F, Faoro A (1985): The EEG of the early premature. Electroencephalogr Clin Neurophysiol 60:95–105.

Andre M, Lamblin MD, d'Allest AM, Curzi-Dascalova L, Moussalli-Salefranque FTSNT, Vecchierini-Blineau MF, Wallois F, Walls-Esquivel E, Plouin P (2010): Electroencephalography in premature and full-term infants. Developmental features and glossary. Clin Neurophysiol 40:59–124.

Ayoub AE, Kostovic I (2009): New horizons for the subplate zone and its pioneering neurons. Cereb Cortex 19:1705–1707.

Azizollahi H, Aarabi A, Wallois F (2016): Effects of uncertainty in head tissue conductivity and complexity on EEG forward modeling. Hum Brain Mapp 37:3604–3622.

Baillet S, Riera JJ, Marin G, Mangin JF, Aubert J, Garnero L (2001): Evaluation of inverse methods and head models for EEG source localization using a human skull phantom. Phys Med Biol 46:77–96.

Biagioni E, Bartalena L, Boldrini A, Cioni G, Giancola S, Ipata AE (1994): Background EEG activity in preterm infants: Correlation of outcome with selected maturational features. Electroencephalogr Clin Neurophysiol 91:154–162.

Carter RM, Huettel SA (2013): A nexus model of the temporal-parietal junction. Trends Cogn Sci 17:328–336.

Chipaux M, Colonnese MT, Mauguen A, Fellous L, Mokhtari M, Lezcano O, Milh M, Dulac O, Chiron C, Khazipov R, Kaminska A (2013): Auditory stimuli mimicking ambient sounds drive temporal "delta-brushes" in premature infants. PloS One 8:e79028.

Chiu C, Weliky M (2001): Spontaneous activity in developing ferret visual cortex in vivo. J Neurosci 21:8906–8914.

Cho JH, Vorwerk J, Wolters CH, Knosche TR (2015): Influence of the head model on EEG and MEG source connectivity analyses. NeuroImage 110:60–77.

Colonnese MT, Kaminska A, Minlebaev M, Milh M, Bloem B, Lescure S, Moriette G, Chiron C, Ben-Ari Y, Khazipov R (2010): A conserved switch in sensory processing prepares developing neocortex for vision. Neuron 67:480–498.

Conhaim J, Easton CR, Becker MI, Barahimi M, Cedarbaum ER, Moore JG, Mather LF, Dabagh S, Minter DJ, Moen SP, Moody WJ (2011): Developmental changes in propagation patterns and transmitter dependence of waves of spontaneous activity in the mouse cerebral cortex. J Physiol 589:2529–2541.

Crowley JC, Katz LC (2000): Early development of ocular dominance columns. Science 290:1321–1324.

Dubois J, Benders M, Cachia A, Lazeyras F, Ha-Vinh Leuchter R, Sizonenko SV, Borradori-Tolsa C, Mangin JF, Huppi PS (2008): Mapping the early cortical folding process in the preterm newborn brain. Cereb Cortex 18:1444–1454.

Dubois J, Dehaene-Lambertz G, Kulikova S, Poupon C, Huppi PS, Hertz-Pannier L (2014): The early development of brain white matter: A review of imaging studies in fetuses, newborns and infants. Neuroscience 276:48–71.

Feller M (2012): Cortical development: The sources of spontaneous patterned activity. Curr Biol: CB 22:R89–R91.

Garaschuk O, Linn J, Eilers J, Konnerth A (2000): Large-scale oscillatory calcium waves in the immature cortex. Nat Neurosci 3:452–459.

Gargiulo P, Belfiore P, Friethgeirsson EA, Vanhatalo S, Ramon C (2015): The effect of fontanel on scalp EEG potentials in the neonate. Clin Neurophysiol 126:1703–1710.

Geddes LA, Baker LE (1967): Chlorided silver electrodes. Med Res Eng 6:33–34.

Goncalves S, de Munck JC, Verbunt JP, Heethaar RM, da Silva FH (2003): In vivo measurement of the brain and skull resistivities using an EIT-based method and the combined analysis of SEF/SEP data. IEEE Trans Biomed Eng 50:1124–1128.

Gonzalez-Islas C, Chub N, Garcia-Bereguiain MA, Wenner P (2010): GABAergic synaptic scaling in embryonic motoneurons is mediated by a shift in the chloride reversal potential. J Neurosci 30:13016–13020.

Hanganu IL, Ben-Ari Y, Khazipov R (2006): Retinal waves trigger spindle bursts in the neonatal rat visual cortex. J Neurosci 26: 6728–6736.

Hughes JR, Fino JJ, Hart LA (1987): Premature temporal theta (PT theta). Electroencephalogr Clin Neurophysiol 67:7–15.

Judas M, Sedmak G, Kostovic I (2013): The significance of the subplate for evolution and developmental plasticity of the human brain. Front Hum Neurosci 7:423.

Kilb W, Kirischuk S, Luhmann HJ (2011): Electrical activity patterns and the functional maturation of the neocortex. Eur J Neurosci 34:1677–1686.

Koessler L, Cecchin T, Caspary O, Benhadid A, Vespignani H, Maillard L (2011): EEG-MRI co-registration and sensor labeling using a 3D laser scanner. Ann Biomed Eng 39:983–995.

Kostovic I, Judas M (2010): The development of the subplate and thalamocortical connections in the human foetal brain. Acta Paediatr 99:1119–1127.

Kostovic I, Judas M, Sedmak G (2011): Developmental history of the subplate zone, subplate neurons and interstitial white matter neurons: Relevance for schizophrenia. Int J Dev Neurosci 29:193–205.

Kostovic I, Sedmak G, Vuksic M, Judas M (2015): The relevance of human fetal subplate zone for developmental neuropathology of neuronal migration disorders and cortical dysplasia. CNS Neurosci Therap 21:74–82.

Kotak VC, Sadahiro M, Fall CP (2007): Developmental expression of endogenous oscillations and waves in the auditory cortex involves calcium, gap junctions, and GABA. Neuroscience 146: 1629–1639.

Kotak VC, Pendola LM, Rodriguez-Contreras A (2012): Spontaneous activity in the developing gerbil auditory cortex in vivo involves GABAergic transmission. Neuroscience 226: 130–144.

Lamblin MD, Andre M, Challamel MJ, Curzi-Dascalova L, d'Allest AM, De Giovanni E, Moussalli-Salefranque F, Navelet Y, Plouin P, Radvanyi-Bouvet MF, Samson-Dollfus D, Vecchierini-Blineau MF (1999): Electroencephalography of the premature and term newborn. Maturational aspects and glossary. Clin Neurophysiol 29:123–219.

Lanfer B, Scherg M, Dannhauer M, Knosche TR, Burger M, Wolters CH (2012): Influences of skull segmentation inaccuracies on EEG source analysis. NeuroImage 62:418–431.

Leroy F, Glasel H, Dubois J, Hertz-Pannier L, Thirion B, Mangin JF, Dehaene-Lambertz G (2011): Early maturation of the linguistic dorsal pathway in human infants. J Neurosci 31: 1500–1506.

Lew S, Sliva DD, Choe MS, Grant PE, Okada Y, Wolters CH, Hamalainen MS (2013): Effects of sutures and fontanels on MEG and EEG source analysis in a realistic infant head model. NeuroImage 76:282–293.

Lischalk JW, Easton CR, Moody WJ (2009): Bilaterally propagating waves of spontaneous activity arising from discrete pacemakers in the neonatal mouse cerebral cortex. Dev Neurobiol 69:407–414.

Mahmoudzadeh M, Dehaene-Lambertz G, Fournier M, Kongolo G, Goudjil S, Dubois J, Grebe R, Wallois F (2013): Syllabic discrimination in premature human infants prior to complete formation of cortical layers. Proc Natl Acad Sci U S A 110: 4846–4851.

Mahmoudzadeh M, Wallois F, Kongolo G, Goudjil S, Dehaene-Lambertz G (2016): Functional maps at the onset of auditory inputs in very early preterm human neonates. Cereb Cortex. In Press.

McAllister AK (1999): Subplate neurons: A missing link among neurotrophins, activity, and ocular dominance plasticity?. Proc Natl Acad Sci U S A 96:13600–13602.

Milh M, Kaminska A, Huon C, Lapillonne A, Ben-Ari Y, Khazipov R (2007): Rapid cortical oscillations and early motor activity in premature human neonate. Cereb Cortex 17: 1582–1594.

Moore JK, Linthicum FH Jr (2007): The human auditory system: A timeline of development. Int J Audiol 46:460–478.

Moore AR, Zhou WL, Jakovcevski I, Zecevic N, Antic SD (2011): Spontaneous electrical activity in the human fetal cortex in vitro. J Neurosci 31:2391–2398.

O'Leary DD, Chou SJ, Sahara S (2007): Area patterning of the mammalian cortex. Neuron 56:252–269.

Odabaee M, Freeman WJ, Colditz PB, Ramon C, Vanhatalo S (2013): Spatial patterning of the neonatal EEG suggests a need for a high number of electrodes. NeuroImage 68:229–235.

Ramon C, Schimpf PH, Haueisen J (2004): Effect of model complexity on EEG source localizations. Neurol Clin Neurophysiol: NCN 2004:81.

Rice JK, Rorden C, Little JS, Parra LC (2013): Subject position affects EEG magnitudes. NeuroImage 64:476–484.

Roche-Labarbe N, Aarabi A, Kongolo G, Gondry-Jouet C, Dumpelmann M, Grebe R, Wallois F (2008): High-resolution electroencephalography and source localization in neonates. Hum Brain Mapp 29:167–176.

Sarnat HB, Flores-Sarnat L (2002): Cajal-Retzius and subplate neurons: Their role in cortical development. Eur J Paediatr Neurol 6:91–97.

Shatz CJ, Ghosh A, McConnell SK, Allendoerfer KL, Friauf E, Antonini A (1990): Pioneer neurons and target selection in cerebral cortical development. Cold Spring Harbor Symp Quant Biol 55:469–480.

Tritsch NX, Bergles DE (2010): Developmental regulation of spontaneous activity in the Mammalian cochlea. J Neurosci 30: 1539–1550.

Tritsch NX, Yi E, Gale JE, Glowatzki E, Bergles DE (2007): The origin of spontaneous activity in the developing auditory system. Nature 450:50–55.

Ulfig N, Neudorfer F, Bohl J (2000): Transient structures of the human fetal brain: Subplate, thalamic reticular complex, ganglionic eminence. Histol Histopathol 15:771–790.

Vallaghe S, Clerc M (2009): A global sensitivity analysis of three- and four-layer EEG conductivity models. IEEE Trans Bio-med Eng 56:988–995.

Vanhatalo S, Tallgren P, Andersson S, Sainio K, Voipio J, Kaila K (2002): DC-EEG discloses prominent, very slow activity patterns during sleep in preterm infants. Clin Neurophysiol 113: 1822–1825.

Vecchierini MF, d'Allest AM, Verpillat P (2003): EEG patterns in 10 extreme premature neonates with normal neurological outcome: Qualitative and quantitative data. Brain Dev 25:330–337.

Vecchierini MF, Leger D, Laaban JP, Putterman G, Figueredo M, Levy J, Vacher C, Monteyrol PJ, Philip P (2008): Efficacy and compliance of mandibular repositioning device in obstructive sleep apnea syndrome under a patient-driven protocol of care. Sleep Med 9:762–769.

Vorwerk J, Cho JH, Rampp S, Hamer H, Knosche TR, Wolters CH (2014): A guideline for head volume conductor modeling in EEG and MEG. NeuroImage 100:590–607.

Wallois F (2010): Synopsis of maturation of specific features in EEG of premature neonates. Clin Neurophysiol 40:125–126.

Weliky M, Katz LC (1999): Correlational structure of spontaneous neuronal activity in the developing lateral geniculate nucleus in vivo. Science 285:599–604.

Wong RO (1999): Retinal waves and visual system development. Annu Rev Neurosci 22:29–47.

Xu HP, Furman M, Mineur YS, Chen H, King SL, Zenisek D, Zhou ZJ, Butts DA, Tian N, Picciotto MR, Crair MC (2011): An

instructive role for patterned spontaneous retinal activity in mouse visual map development. Neuron 70:1115–1127.

Yang JW, Hanganu-Opatz IL, Sun JJ, Luhmann HJ (2009): Three patterns of oscillatory activity differentially synchronize developing neocortical networks in vivo. J Neurosci 29: 9011–9025.

Zanow F, Knosche TR (2004): ASA–Advanced Source Analysis of continuous and event-related EEG/MEG signals. Brain Topogr 16:287–290.

Zhao C, Kao JP, Kanold PO (2009): Functional excitatory microcircuits in neonatal cortex connect thalamus and layer 4. J Neurosci 29:15479–15488.